Continuum Mech. Thermodyn. 1 (1989) 73-80

Continuum Mechanics and Thermodynamics

Moment-curvature relations for a pseudoelastic beam

T. Atanacković and **M. Achenbach**

Pseudoelastic bodies have very simple stress-strain diagrams for uniaxial tensile and compressive loading. In particular, yield and recovery occur at fixed stresses. And yet, the moment-curvature diagrams for bending and unbending of a beam are fairly complex, because the stress and strain fields are non-uniform. The paper shows stress profiles within the beam for pure bending and arrives at explicit equations for loading and unloading curves.

1 Introduction

In some temperature range shape memory alloys exhibit pseudoelasticity. In that range the stress-strain curve of a single crystal under tension and compression has the form shown in Fig. 1. There is a yield limit and a recovery limit so that in a loading–unloading experiment the state of the body runs through

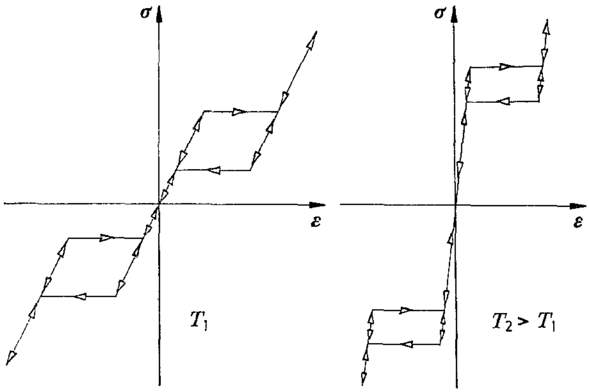

Fig. 1. Stress-strain diagrams for a pseudoelastic body

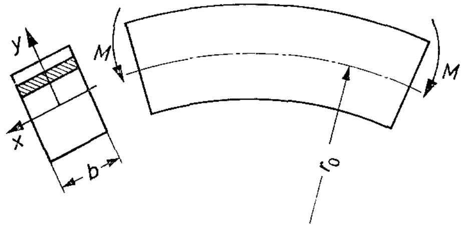

Fig. 2. Dimensions of a beam segment. Coordinates. r_0 is the radius of curvature

a hysteresis loop. At a higher temperature the hysteresis loops are farther away from the origin and altogether smaller.

Given a stress-strain diagram of the type shown in Fig. 1 we shall in this paper derive a moment curvature relation for a pseudoelastic beam in bending. As a result of the non-uniformity of the stress- and strain-fields in the beam this relation will be considerably more complex than the (σ, ε)-relation. We note that in [1] the moment-curvature diagram was assumed to have the same general characteristics as the (σ, ε)-diagrams of Fig. 1. The cross section of the beam is assumed to be rectangular. Its dimensions are shown in Fig. 2 along with the choice of coordinates for the subsequent analysis.

2 Pure bending and unbending of a rectangular beam

We redraw a (σ, ε)-diagram for a memory alloy in the pseudoelastic range in Fig. 3 and introduce some notation that will frequently be referred to in the sequel.

The yield in loading starts at the point $(\sigma_2, \varepsilon_2)$ and ends at $(\sigma_2, \varepsilon_4)$. In unloading from a strain $\varepsilon > \varepsilon_4$ and yield starts at $(\sigma_1, \varepsilon_3)$ and ends at $(\sigma_1, \varepsilon_1)$. If the unloading starts from $\varepsilon_2 < \varepsilon < \varepsilon_4$ (say from point R) it proceeds along the line $\overline{RR^{\mathrm{II}}}$ then $\overline{R^{\mathrm{II}}S}$ and finally $\overline{S0}$. The lines $\overline{0B}$ and $\overline{RR^{\mathrm{II}}}$ are assumed to be parallel

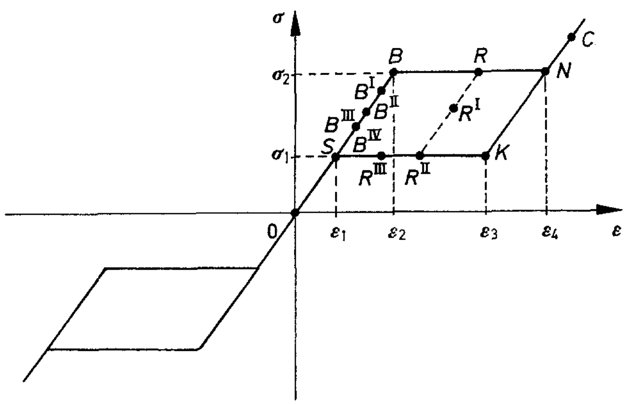

Fig. 3. (σ, ε)-diagram with characteristic points

with the slope E_1. The slope of the line $\overline{CK}$ is $E_2 = E_1$. We assume that the plane sections of an initially straight rod remain plane in the deformed state. Then we know from elementary beam theory that the strain ε in a layer whose distance is y from the neutral axis is given by

$$\varepsilon = \frac{1}{r_0} y = \Phi y, \tag{1}$$

where r_0 is the radius of curvature of the neutral surface and is the curvature itself. For a given ε_1, ε_2, ε_3 and ε_4 we define

$$\Phi_1 = \frac{2}{H}\varepsilon_1; \quad \Phi_2 = \frac{2}{H}\varepsilon_2; \quad \Phi_3 = \frac{2}{H}\varepsilon_3; \quad \Phi_4 = \frac{2}{H}\varepsilon_4. \tag{2}$$

Note that in loading the yield starts in the outer layer of the rod when $\Phi = \Phi_2$ i.e., when a point in the outer layer of the rod reaches point B. The yield region develops up to the point N as Φ increases, that is up to the point when the curvature is $\Phi = \Phi_4$. If $\Phi > \Phi_4$ the state of the outer layer is given by a point, say C, on the right elastic range of the $\sigma - \varepsilon$ diagram. Thus, the stress distribution across the beam has the form shown in Fig. 4.

The position of the layer on the outer border of the elastic core we find from the condition $\varepsilon(y_e) = \Phi y_e = \varepsilon_2$. Thus,

$$y_e = \frac{H}{2}\frac{\Phi_2}{\Phi}. \tag{3}$$

Similarly, for $\Phi > \Phi_4$ the position of the inner border of the outer elastic region $\bar{y}$ is determined from the condition $\varepsilon(\bar{y}) = \varepsilon_4$, or

$$\bar{y} = \frac{H}{2}\frac{\Phi_4}{\Phi}. \tag{4}$$

The bending moment that corresponds to the deformed rod with curvature Φ we find as

$$M = \int_A \sigma y \, dA, \tag{5}$$

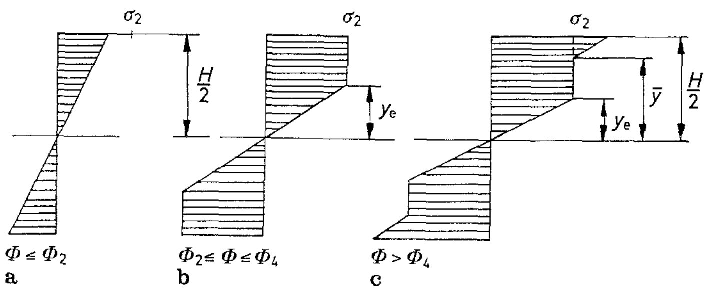

Fig. 4a–c. Stress distribution in loading

where A is the cross-sectional area of the rod. From Fig. 4 and by using (3) and (4) we get that for loading $(M = \overline{M})$

$$\overline{M} = \begin{cases} E_1 I\Phi \quad 0 \leqq \Phi \leqq \Phi_2 \\ E_1 I \left\{\Phi \left(\frac{\Phi_2}{\Phi}\right)^3 + \frac{3}{2}\,\Phi_2 \left[1 - \left(\frac{\Phi_2}{\Phi}\right)^2\right]\right\} \quad \Phi_2 < \Phi \leqq \Phi_4 \\ I\Phi \left\{E_1 \left(\frac{\Phi_2}{\Phi}\right)^3 + E_2 \left[1 - \left(\frac{\Phi_4}{\Phi}\right)^3\right]\right\} + \frac{3}{2}\,E_1 \frac{I[\Phi_4^2 - \Phi_2^2]}{\Phi^2}\,\Phi_2 \\ + \frac{3}{2}\,I \left[1 - \left(\frac{\Phi_4}{\Phi}\right)^2\right] \{E_1\Phi_2 - E_2\Phi_4\} \quad \Phi > \Phi_4, \end{cases} \tag{6}$$

where $I = bH^3/12$ is the axial moment of inertia.

Now we analyse the unloading of the rod. Let Φ_i be the initial curvature, i.e. the curvature when the unloading begins. If $\Phi_i \in [\Phi, \Phi_2]$ then the whole cross section is elastically deformed, the stress distribution is shown in Fig. 4a, and we have for unloading $(M = \hat{M})$

$$\hat{M} = E_1 I\Phi \quad 0 \leqq \Phi \leqq \Phi_2. \tag{7}$$

Now, suppose that $\Phi_i \in [\Phi_2, \Phi_4]$ so that the stress-strain state of a point in the outer layer is given by point R in Fig. 3. To the point on the edge of the elastic core there corresponds the point B. In unloading, when the curvature changes by $-\Delta\Phi$, the change in strain of the points B and R is

$$(\Delta\varepsilon)_B = -\Delta\Phi\, y_e; \quad (\Delta\varepsilon)_R = -\Delta\Phi\,\frac{H}{2}. \tag{8}$$

Since unloading from both points B and R proceeds along lines that are parallel, it follows that the changes in stress at B and R are

$$(\Delta\sigma)_B = -E_1\,\Delta\Phi\, y_e > (\Delta\sigma)_R = -E_1\,\Delta\Phi\,\frac{H}{2}. \tag{9}$$

Thus, the stress distribution across the upper part of the rod will have the form shown in Fig. 5b.

When in unloading the outer layer reaches the point R'', the stress remains constant with the value σ_1 (Fig. 5d). As unloading proceeds, the outer layer of the elastic core reaches point S so that yielded region has a constant stress equal to σ_1 (Fig. 5e).

Further unloading extends the elastic core so that, finally, the state of the outer layer is given by point S. After that, the unloading proceeds as in a lineary elastic body.

To calculate the moments corresponding to the stress distribution shown in Fig. 5, we start with $\Phi_i \in [\Phi_2, \Phi_4]$. The stress at the point B' is given by

$$\sigma_{B'} = E_1\varepsilon_{B\mathrm{I}} = E_1\Phi y_{B\mathrm{I}} = E_1\Phi\,\frac{H}{2}\,\frac{\Phi_2}{\Phi_i}. \tag{10}$$

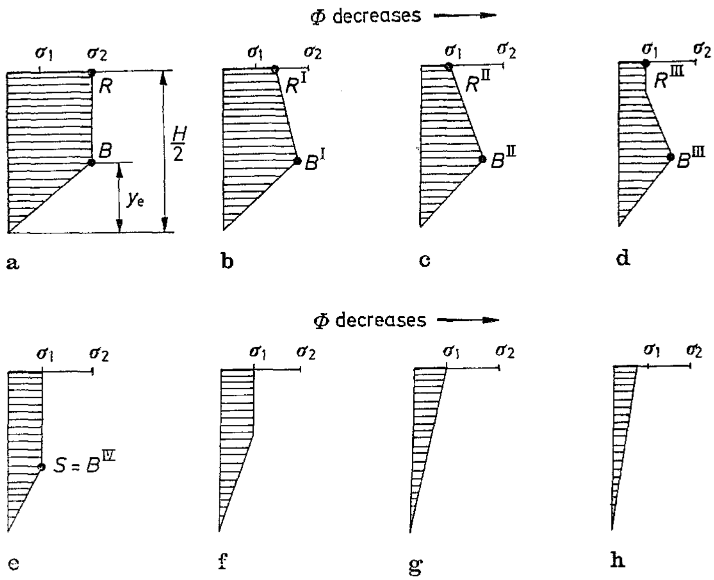

Fig. 5a–h. Stress distributions in unloading

Similarly

$$\sigma_{R\mathrm{I}} = \sigma_2 - (\Delta\varepsilon)_R\, E_1 = E_1 \frac{H}{2}\, [\Phi_2 - (\Phi_i - \Phi)]. \tag{11}$$

With (10) and (11) we can calculate the moment $M = \hat{M}$ by using (5). The result is

$$\hat{M} = E_1 I \left\{ \Phi - \Phi_i \left[1 - \left(\frac{\Phi_2}{\Phi_i} \right)^3 \right] + \tfrac{3}{2}\, \Phi_2 \left[1 - \left(\frac{\Phi_2}{\Phi_i} \right)^2 \right] \right\}. \tag{12}$$

The expression (12) holds until the outer layer reaches state R^{II}. Using (11) we conclude that the expression (12) is valid for

$$\Phi_i - (\Phi_2 - \Phi_1) < \Phi \leqq \Phi_i \leqq \Phi_4. \tag{13}$$

By similar analysis, that we omit, it follows that

$$\hat{M} = \begin{cases} E_1 I \left\{ \Phi - \Phi_i \left[1 - \left(\frac{\Phi_2}{\Phi_i} \right)^3 \right] + \tfrac{3}{2} \left[1 - \left(\frac{\Phi_2}{\Phi_i} \right)^2 \right] \right\} \\ \Phi_i - (\Phi_2 - \Phi_1) < \Phi \leqq \Phi_i \leqq \Phi_4 \\ E_1 I \left\{ \tfrac{1}{2} \frac{(\Phi_2 - \Phi_1)^3}{(\Phi_i - \Phi)^2} + \tfrac{3}{2}\, \Phi_1 - \tfrac{1}{2} \frac{\Phi_2^3}{\Phi_i^2} \right\} \\ \Phi_i \frac{\Phi_1}{\Phi_2} \leqq \Phi \leqq \Phi_i - (\Phi_2 - \Phi_1) \\ E_1 I \left\{ \tfrac{3}{2}\, \Phi_1 - \tfrac{1}{2} \frac{\Phi_1^3}{\Phi^2} \right\} \qquad \Phi_1 \leqq \Phi \leqq \Phi_i \frac{\Phi_1}{\Phi_2} \\ E_1 I \Phi \qquad 0 \leqq \Phi \leqq \Phi_1 . \end{cases} \tag{14}$$

Finally, we consider the case when the unloading begins at the value of $\Phi_i > \Phi_4$. The stress-strain state of a point in the outer layer corresponds to the point C. The stress distribution is shown in Fig. 4c. Thus, from (6) we have

$$\begin{aligned}\hat{M} = I\Phi \left\{E_1 \left(\frac{\Phi_2}{\Phi}\right)^3 + E_2 \left[1 - \left(\frac{\Phi_4}{\Phi}\right)^3\right]\right\} \\ + \tfrac{3}{2} E_1 I \left[\frac{\Phi_4^2 - \Phi_2^2}{\Phi^2}\right] \Phi_2 \\ + \tfrac{3}{2} I[E_1\Phi_2 - E_2\Phi_4] \left[1 - \left(\frac{\Phi_4}{\Phi}\right)^2\right],\end{aligned} \tag{15}$$

for $\Phi_4 \leqq \Phi \leqq \Phi_i$. When, in unloading, Φ reaches Φ_4, the unloading follows the sequence shown in Fig. 5. Therefore for $\Phi \leqq \Phi_4$ the moment $\hat{M}$ is determined by (14) with $\Phi_i = \Phi_4$.

We make two remarks concerning the formula for loading $\overline{M}(\Phi)$ and unloading $\hat{M}(\Phi)$. If the rod is not straight initially but has a constant curvature Φ_0 the argument in $\overline{M}$ and $\hat{M}$ instead of Φ should be $\Phi - \Phi_0$. Also it is obvious from the expressions for $\overline{M}$ and $\hat{M}$ that both depend on the cross section. Formula similar to (6), (14) and (15) could be easily derived for other cross sections.

In Fig. 6 we show characteristic loading $\overline{M}$ and unloading $\hat{M}$ curves.

If the temperature of the rod is increased, say from T_1 to T_2, then the initial modul of elasticity is increased from $E_1^{①}$ to $E_1^{②}$. Thus, from (6) we have

$$\overline{M}_2(\Phi) > \overline{M}_1(\Phi). \tag{16}$$

Thus in conclusion we say that the (M, Φ)-diagram for bending is fairly complex, even thought the (σ, ε)-diagram for tensile and compressive loading consists only of straight lines. This fact must be taken into account, if one wishes to extract information on constitutive properties from bending experiments.

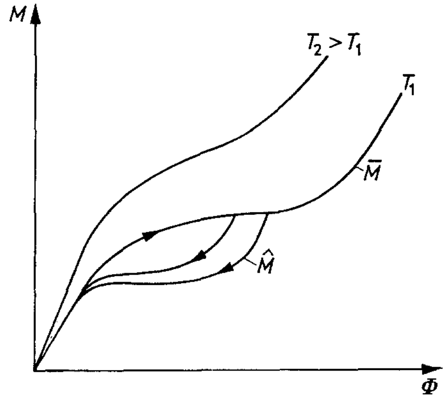

Fig. 6. Moment curvature relations for loading and unloading

As a special point of interest we mention that in bending of a pseudoelastic beam the layers subject to maximal stress need not be the outer ones. This is put in evidence by the Fig. 5b through 5d.

3 An application

Now we use the results of the previous section to estimate the driving moment of a thermobile [2]. We assume that the thermobile works between moderately high temperatures so that the stress-strain diagram has the form shown in Fig. 3. A thermobile consists of two wheels and a memory wire around them, see Fig. 7. The cold wire coming to the lower wheel of radius r is bent at the point ① from $\Phi = 0$ to $\Phi = 1/r$ along the curve $\overline{M}_1$ in Fig. 8. While in contact with hot water (from points ① to ②) the wire is heated with the curvature remaining constant. The point ② belongs to the loading curve $\overline{M}_2$ at the higher temperature. At the point ③ the wire becomes straight again ($\Phi = 0$). That means that from ② to ③ the state of the wire changes along the unloading curve $\hat{M}_2$ (Fig. 8).

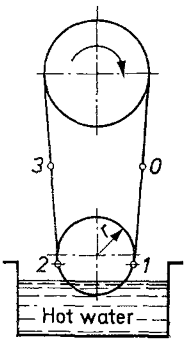

Fig. 7. Schematic view of a thermobile

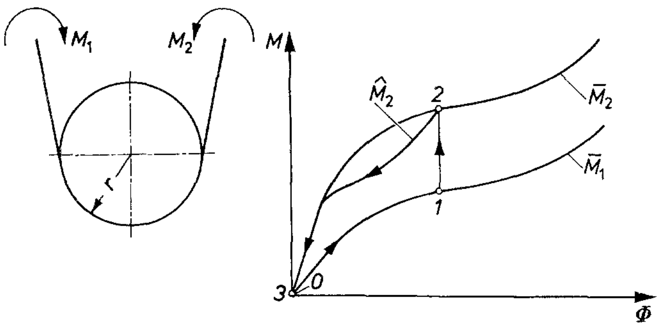

Fig. 8. The thermobile processes in (M, Φ) diagram

The moment that produces rotation of the wheels is

$$\Delta M = \hat{M}_2 \left(\frac{1}{r}\right) - \overline{M}_1 \left(\frac{1}{r}\right). \tag{17}$$

Its value may be calculated using (5), (14) and (15), if the properties of the wire are known.

Acknowledgement: The financial support of Alexander von Humboldt-Foundation to T. Atanacković during the course of this work is most gratefully acknowledged.

References

1. James, R. D.: The equilibrium and postbuckling behavior of an elastic curve governed by a nonconvex energy. J. Elasticity 11 (1981) 239–269
2. Wang, F. E.: The thermobile nitinol engine. MECCA, Milwaukee, Wisconsin SAE Technical Paper (1985) 1–9

T. Atanacković
Fakultet Technickih Nauka
Veljka Vlahovica 3
21000 Novi Sad
Yugoslavia

M. Achenbach
Hermann Föttinger Institut
Technische Universität
D-1000 Berlin 12

Received September 12, 1988